

**Are your MRI contrast agents cost-effective?**

Learn more about generic Gadolinium-Based Contrast Agents.



**FRESENIUS  
KABI**

caring for life

**AJNR**

## **Modified Histologic Technique for Processing Metallic Coil-Bearing Tissue**

Daying Dai, Yong Hong Ding, Mark A. Danielson,  
Ramanathan Kadirvel, Debra A. Lewis, Harry J. Cloft and  
David F. Kallmes

This information is current as  
of December 7, 2024.

*AJNR Am J Neuroradiol* 2005, 26 (8) 1932-1936  
<http://www.ajnr.org/content/26/8/1932>

## Modified Histologic Technique for Processing Metallic Coil-Bearing Tissue

Daying Dai, Yong Hong Ding, Mark A. Danielson, Ramanathan Kadirvel, Debra A. Lewis, Harry J. Cloft, and David F. Kallmes

**We developed a modified paraffin-embedding histologic technique for processing metallic coil-bearing aneurysm tissues. This modified technique was successfully employed for processing platinum coil-bearing tissue for 30 rabbit aneurysms and 6 swine aneurysms. This technique for sectioning coil-bearing aneurysms resulted in little or no tissue distortion and permitted good preservation of morphology and application of multiple advanced staining techniques. This technique is considered beneficial for studying the molecular mechanisms of aneurysm healing after coiling.**

Histopathologic studies of aneurysms treated by coil embolization are hampered by the presence of metallic material. The advanced techniques that allow for the characterization of cells and tissues found after embolization of experimental aneurysms were seldom reported. As such, the currently available histologic data have been insufficient to identify the aneurysms' healing mechanism following coil embolization, and the details of the cellular and biologic reaction to the coil implantation have remained clouded.

Most studies examining aneurysms' histology after coiling have used a plastic-embedding technique (1–5). The hardness differential between the paraffin and the platinum coils results in massive distortion of the sectioned samples embedded in paraffin. Plastics minimize this differential. Typically, after plastic embedding, samples are cut into “macro” sections (~1 mm), which are ground by using precision grinders to yield wafers (~30  $\mu$ m), thin enough to permit light penetration.

Plastic-embedding techniques, though useful to prevent tissue distortion, have substantial drawbacks. The heat liberated during the exothermic plastic-embedding process may denature proteins that would otherwise be useful for immunostains. Also, relatively few sections, compared with paraffin, are obtained; most of the tissue is ground away. Finally, good stain penetration, even for standard stains, may be impeded by imperfect removal of plastic.

We herein report a modified technique by which platinum coil-bearing tissues can be processed via paraffin embedding. This technique secures good

preservation of morphology, as well as multiple, thin sections that are easily stained with regular and advanced histologic staining techniques.

### Materials and Methods

The Institutional Animal Care and Use Committee at the Mayo Clinic approved all procedures. A sterile technique was employed for all procedures.

#### *Rabbit Saccular Aneurysm Model*

Elastase-induced, saccular aneurysms were created in New Zealand white rabbits (3–4 kg in weight). Detailed procedures for this model have been described elsewhere (6). In brief, animals were anesthetized, the right common carotid artery (CCA) was exposed, and porcine elastase (Worthington Biochemical Corporation, Lakewood, NJ) was incubated within the lumen to create an aneurysm.

#### *Rabbit Aneurysm Embolization Procedure*

Aneurysms matured for a minimum of 21 days following creation. Animals were anesthetized, and a cutdown was performed to gain access to the right common femoral artery (CFA). A microcatheter was inserted coaxially through the guiding catheter into the aortic arch. Aneurysms were embolized with platinum coils via the microcatheter (4). Aneurysm cavities were densely packed in all cases. Final digital subtraction angiograms (DSAs) were performed following embolization.

Aneurysms were harvested at 2 ( $n = 4$ ), 4 ( $n = 8$ ), 10 ( $n = 6$ ), 16 ( $n = 6$ ), and 24 weeks ( $n = 6$ ). At sacrifice, animals were deeply anesthetized and then sacrificed with a lethal injection of pentobarbital. The chest cavity was opened, and a rapid injection of saline and formalin flushed the aortic arch and the coil-embolized aneurysm. Specimens were removed and immediately fixed in 10% neutral-buffered formalin for at least 24 hours.

#### *Porcine Sidewall Aneurysm Model*

Sidewall aneurysms were created in domestic swine (30–40 kg) by using the methods of German and Black (7). In brief, the right external jugular vein was exposed and isolated. Two

Received January 5, 2005; accepted after revision March 27.

From the Department of Radiology, Mayo Clinic, Rochester, MN.

Address correspondence to David F. Kallmes, MD, Department of Radiology, Mayo Clinic, 200 First Street, SW, Rochester, MN 55905.

pieces of vein (~4 cm) were harvested and placed in sterile saline. A carotid arteriotomy (~7 mm in diameter) was made, and an end-to-side anastomosis was performed. Following this procedure, blood flow was reestablished, resulting in an aneurysm.

#### *Swine Embolization Procedure*

Porcine embolization proceeded as described elsewhere (4). In brief, a cutdown was performed to gain access to the right CFA. A microcatheter was inserted coaxially through the guiding catheter into the midright CCA. Dimensions of the aneurysm were determined with external sizing markers via DSA. Platinum coil was placed into the aneurysm through the microcatheter. All were densely packed.

Aneurysms were harvested at 1 ( $n = 2$ ) and 12 weeks ( $n = 4$ ). Animals were deeply anesthetized and then were sacrificed by using a lethal injection of pentobarbital. The CCAs, including the aneurysms with coils, were dissected from surrounding tissue, removed, and placed in 10% neutral-buffered formalin.

#### *Tissue-Processing Procedure*

Specimens were fixed in 10% neutral-buffered formalin for 105 minutes. They were then placed in alcoholic formalin for 2 hours, followed by 70% alcohol for 30 minutes, 80% alcohol for 30 minutes, 2 changes of 95% alcohol (30 minutes each), and 2 changes of 100% alcohol (55 minutes each). Next, specimens were placed in 2 changes of Xylene (55 minutes each), followed by 3 changes of liquid paraffin (40 minutes each). Finally, specimens were embedded in rectangular paraffin blocks. Vacuum and heat were employed during tissue processing.

The aneurysms were sectioned with an Isomet Low Speed saw (Buehler, Lake Bluff, IL; series 15HC Diamond Blade) at 1000- $\mu$ m intervals in a coronal orientation, permitting long-axis sectioning of the aneurysm neck. Coil fragments were carefully removed with forceps under a dissection microscope. Following removal of all fragments, the sections were reembedded in paraffin blocks. A microtome (Leica Microsystems, Nussloch, Germany, model RM2165) with disposable blades sectioned the blocks at 5–6- $\mu$ m intervals. Sections were floated in a water bath (42°C) and then mounted on Superfrost Plus slides (Fisher Scientific International, Hampton, NH) and dried overnight in an oven (37°C).

#### *Staining*

**Hematoxylin and Eosin.** At minimum, 2 sections from each block were stained with hematoxylin and eosin (H&E) for conventional histopathologic evaluation. Slides were deparaffinized and hydrated in water, followed by staining with hematoxylin (3–5 minutes). Slides were stained with eosin for 1–2 minutes and then quickly dehydrated in graded alcohol solutions, cleared with xylene, and mounted with EZ-Mount (ThermoShandon, Pittsburgh, PA).

**Masson Trichrome.** Serial sections were stained with Masson Trichrome (Masson) for collagen assessment. Slides were deparaffinized and hydrated in distilled water (DH<sub>2</sub>O), then placed in a water bath (56°C) with Bouin's solution (Sigma-Aldrich, St. Louis, MO) for 30 minutes. They were stained for 10 minutes with filtered Weight iron hematoxylin working solution (Sigma-Aldrich) and washed in tap water (5 minutes). After rinsing in DH<sub>2</sub>O, they were stained in Sigma Biebrich Scarlet Acid Fuchsin (4 minutes) and rinsed in DH<sub>2</sub>O. They were placed in phosphomolybdic-phosphotungstic acid (Sigma) working solution for 12 minutes followed by 20 minutes in Aniline Blue (Polysciences, Warrington, PA) solution. Finally, after rinsing in DH<sub>2</sub>O, they were placed in 1% acetic acid (4 minutes), dehydrated through alcohols, cleared in xylene, and mounted with EZ-Mount.

**Immunohistochemical staining.** The Vectastain Elite ABC system (Vector Laboratories, Burlingame, CA) was employed.

Primary antibodies used included monoclonal mouse anti-smooth muscle actin (SMA, 1:200; DakoCytomation, Carpinteria, CA), mouse monoclonal antimyosin smooth (myosin heavy chain clone HSM-V 1:1000; Sigma), mouse monoclonal antidesmin (clone DE-U-10, 1:150; Sigma), and mouse monoclonal antivimentin (clone LN-6, 1:200; Sigma). Sections were dried (56°C) for 1–2 hours and then deparaffinized and hydrated in alcohol solutions of 100%, 95%, and 80% and in distilled water. Incubation in hydrogen peroxide (0.3% in DH<sub>2</sub>O; 20 minutes) followed. Sections were pretreated with 0.1 mol/L citric acid buffer and microwaved for 15 minutes. Slides cooled at room temperature (30 minutes) and then were rinsed in phosphate-buffered saline (PBS). Sections were incubated with normal 5% horse serum (20 minutes; 37°C), followed by incubation with the appropriate primary antibody (1 hour). Slides were rinsed in PBS and incubated (37°C; 1 hour) with biotinylated secondary horse antimouse IgG (Vector Laboratories). Sections were rinsed in PBS and incubated with Vectastain Elite ABC Reagent (Vector Laboratories) for 45 minutes at 37°C. Finally, slides were stained with diaminobenzidine-tetrahydrochloride substrate kit (Vector Laboratories) for horseradish peroxidase and counter stained with Gill hematoxylin (Sigma Diagnostics). Positive controls included sections of human coronary arteries that were positive for SMA, myosin, desmin, and vimentin. Negative controls were performed with nonimmune, normal serum in place of the primary antibody.

#### *Histologic Analysis*

Two experienced observers independently reviewed all the slides by using an Olympus BH2 microscope (Olympus, Melville, NY). Images were recorded with a Spot RT digital camera (version 3.0; Diagnostic Instruments, Sterling Heights, MN).

#### *Tissue Distortion*

H&E-stained slides were reviewed and graded for tissue distortion as follows: (1) no distortion (coil winds and neck perfectly preserved); (2) mild distortion (less than one-third inside aneurysm dome with tissue distortion or less than one-third of neck absent); (3) moderate distortion (between one-third and two-thirds of the aneurysm dome or neck absent); severe distortion (more than two-thirds of dome or neck absent). The rate of tissue distortion in samples from 2–4 weeks (early samples) was compared with that in samples from 10–24 weeks (late samples) by using the Fisher exact test. A  $P$  value  $< .05$  on 2-sided tests was considered to be statistically significant.

## **Results**

#### *Tissue Distortion*

Thirty-six coiled aneurysms were examined in this study, which included 30 elastase-induced aneurysms in rabbits and 6 surgically created, sidewall aneurysms in swine. Thirty-two (89%) of 36 specimens demonstrated no tissue distortion. Four (11%) specimens showed mild tissue distortion. In the 30 elastase-induced aneurysms, 2/4 samples harvested at 2 weeks showed mild dome tissue distortion; the other 2 samples at this time point demonstrated the dome and neck tissues were preserved well without distortion (Fig 1). Two of 8 (25%) aneurysm samples harvested at 4 weeks displayed mild tissue distortion within the aneurysm and at the neck. No tissue distortion was present on the samples at 10-, 16-, and 24-week time

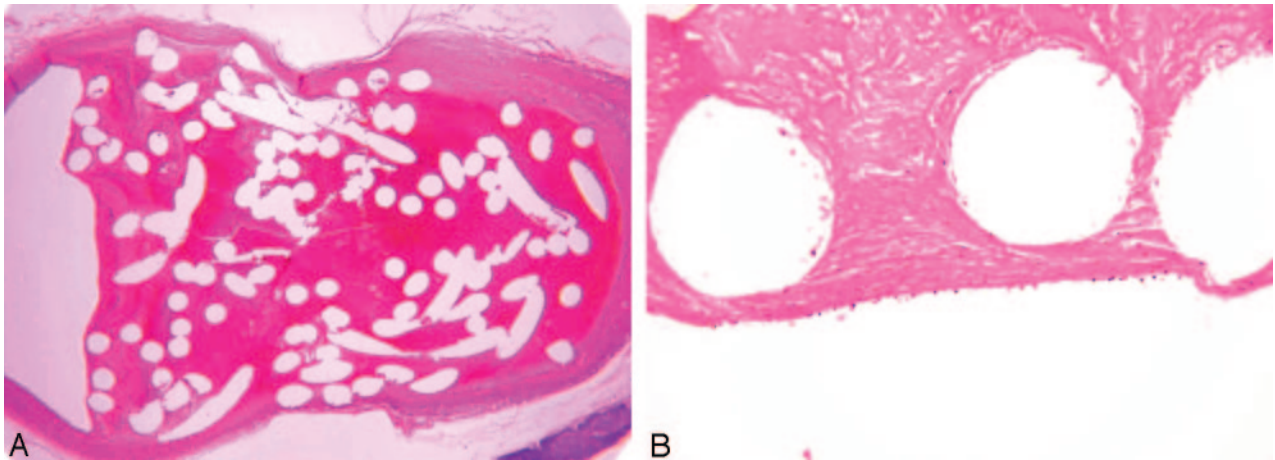


FIG 1. Rabbit aneurysm, 2 weeks postembolization.

A, Photomicrograph shows unorganized thrombus within the aneurysm cavity and across the aneurysm neck. Excellent tissue preservation was achieved in this setting of friable thrombus. (H&E; original magnification, 20 $\times$ ).

B, Higher magnification of aneurysm neck shown in panel A. Photomicrograph shows no endothelial cell coverage at aneurysm neck (H&E; original magnification, 100 $\times$ ).

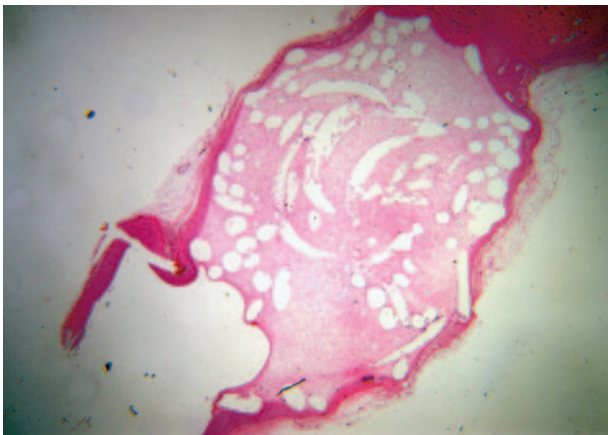


FIG 2. Rabbit aneurysm, 10 weeks postembolization, illustrates loose connective tissue completely filling the aneurysm's cavity; thin layer of tissue covered with single layer of endothelial cells traverses the entire neck. Excellent tissue preservation is achieved within the dome and at the neck (H&E; original magnification, 15 $\times$ ).

points (Fig 2). No specimens at any time point had moderate or severe tissue distortion. There was more distortion in the earlier samples (2–4 weeks) compared with samples from the late time points (10–24 weeks) ( $P = .018$ ; Fisher exact test).

Tissue within dome and at neck were well preserved without distortion in all 6 swine samples (Fig 3). Masson trichrome and immunohistochemistry for multiple antibodies were successfully performed on all rabbit and swine samples (Figs 4 and 5).

#### Regular Histopathologic Evaluation

**Aneurysms in rabbits.** Two weeks after embolization, the primary pathologic feature in the dome was unorganized thrombus. Endothelial coverage at the neck was absent in all 4 samples (Fig 1). Four weeks after embolization, loose connective tissue with

neovessels were present within the aneurysm dome, accompanied by at least a portion of unorganized thrombus in 7 samples. A single, small sample displayed completely organized loose tissue within the dome and a layer of endothelial cell coverage at the aneurysm neck. Ten weeks and later following embolization, hypocellular, loose connective was the main histologic change in the dome, and a thin layer of hypocellular fibrous tissue with entire endothelial cell coverage across the neck was easily found.

**Swine histology.** One week after embolization, both specimens displayed unorganized thrombus filling the entire dome and traversing the entire neck of aneurysm (Fig 3). Twelve weeks after embolization, 2 samples showed attenuated chronic inflammatory tissue completely filling the aneurysm domes. The other 2 specimens had attenuated fibrous connective tissue with numerous thin-walled vessels completely filling the aneurysm lumens; numerous elongated spindle cells embedded in the attenuated fibrous were noted. All 4 samples demonstrated very thick, hypercellular tissue traversing the entire neck, which was covered with a single layer of endothelial cells that was contiguous with the endothelium of the parent artery.

#### Discussion

This study demonstrated a novel, modified histologic technique for paraffin embedding, sectioning, and staining of coil-containing aneurysms. This technique successfully permitted very thin sections ( $\sim 5 \mu\text{m}$ ) to be obtained routinely. Also, well-preserved histomorphologic information was obtained in most samples. Data showing tissue distortion were unusual and restricted to early rabbit time points. Tissue distortion was absent in long-term samples in rabbits and in all time points in swine.

We found that the early time point rabbit specimens exhibited large degrees of unorganized thrombus, which rendered the tissue difficult to handle.

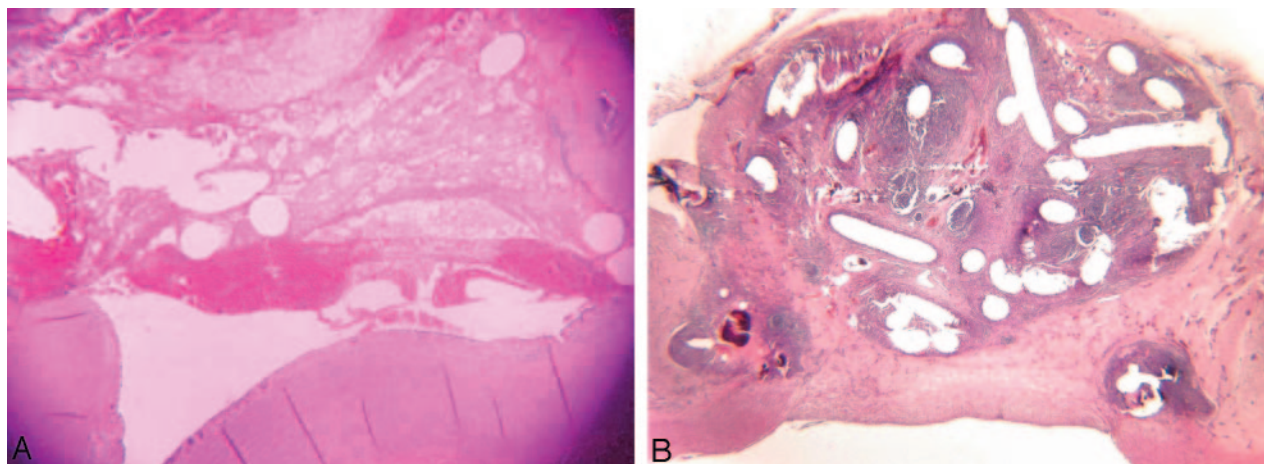


FIG 3. Swine aneurysms, 1 week (A) and 12 weeks (B) postembolization.

A, Photomicrograph shows the unorganized thrombus without endothelial cell infiltration across the entire neck (H&E; original magnification, 40 $\times$ ).

B, Photomicrograph reveals substantial, chronic inflammatory changes in the dome, and a thick layer of hypercellular tissue across the aneurysm's neck (H&E; original magnification, 20 $\times$ ). Excellent tissue preservation is achieved in both early and late time samples.

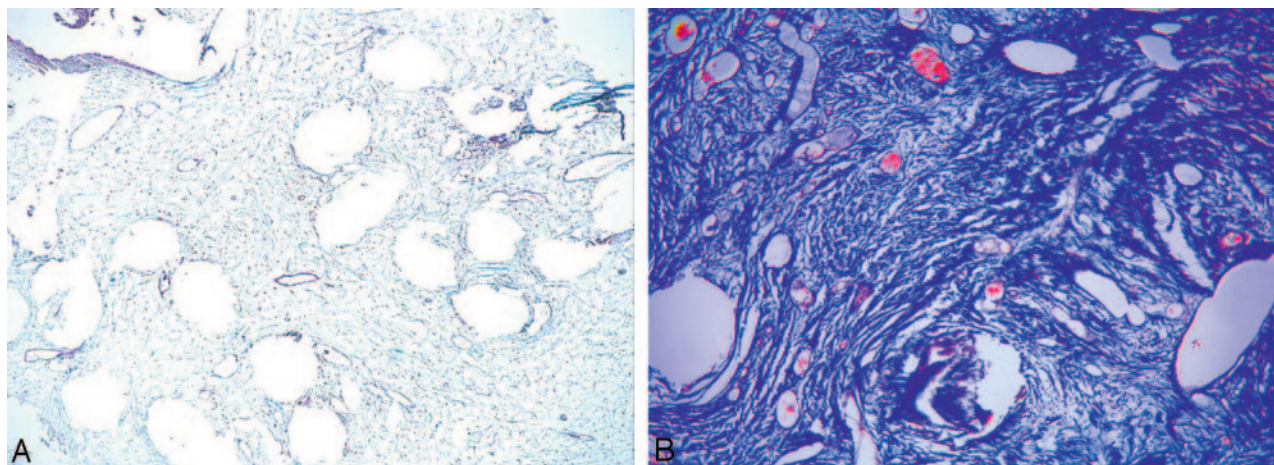


FIG 4. Rabbit aneurysm, 16 weeks postembolization (A), and swine aneurysm, 12 weeks postembolization (B). Photomicrographs show Masson trichrome was successfully performed on both species. A, Masson trichrome; original magnification, 40 $\times$ . B, Masson trichrome; original magnification, 60 $\times$ .

Tissue easily dropped off the section while the low-speed saw was used or during coil removal under the dissecting microscope. Increasing the thickness of section while cutting with the low-speed saw ameliorated this difficulty.

The paraffin technique was successful because it permitted advanced, multiple staining techniques, such as detailed immunohistochemical analysis of intact tissue, something seldom reported for coil-embolized aneurysms. This makes the in situ analysis of histology and cellular molecular biology for these aneurysms possible. This technique permitted multiple sections (as many as 1000 sections per sample) to be obtained from the same sample. These specimens can be kept at 4 $^{\circ}$ C for long periods of time. Thus, when new experimental techniques become available or when techniques need to be repeated samples are available, the use of advanced histology techniques

can potentially improve our understanding of aneurysms' healing mechanisms and what modifications to coils will promote these mechanisms.

This modified technique enabled us to employ detailed immunohistochemistry, immunofluorescence, and TUNEL (data not shown) on a large number of specimens. Techniques permitted a longitudinal description of aneurysm response to endovascular coil embolization via extracellular matrix deposition and cellular responses, which may be addressed with the modification of new vascular devices.

This modified histologic technique has prospectively been employed to human brain aneurysm tissue (D. Dai and D.F. Kallmes, unpublished data). The modified paraffin technique allowed us to apply multiple histologic techniques to explore the cellular reaction to platinum coils on human tissue. Currently, the sections from the modified techniques are being

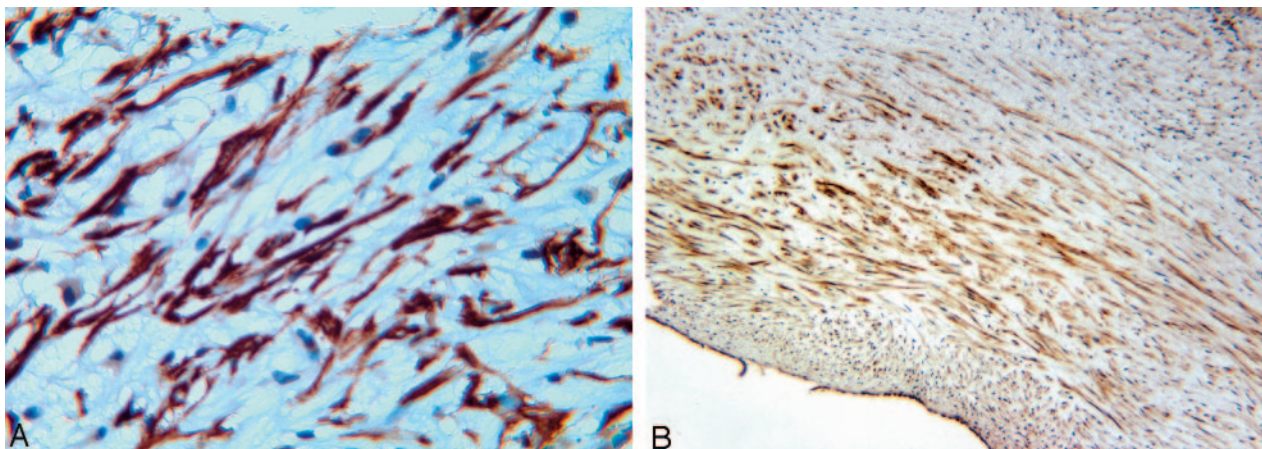


FIG 5. Rabbit aneurysm, 4 weeks postembolization (A), and swine aneurysm, 12 weeks postembolization (B). Photomicrographs show immunohistochemistry was successfully performed on coiled rabbit and swine tissues. Brown signal intensity localized within the spindle cells' cytoplasm indicates positive staining. A, Antibody for Alpha smooth muscle actin antibody; original magnification, 400 $\times$ . B, Antibody for desmin antibody; original magnification, 150 $\times$ .

employed for laser capture microscope and in situ hybridization to identify the molecular biology of these cells, which are involved in the healing of aneurysms; these works are ongoing in our lab. We have moved to exclusive use of paraffin, rather than plastic, for all of our work and are pleased with the results.

### Conclusion

We reported a modified paraffin-embedding histologic technique, which was successful for sectioning coil-bearing aneurysms. The technique permits both good preservation of histologic morphology and the application of multiple, advanced staining techniques to clarify the cellular and molecular mechanisms of coil embolization.

### References

1. Dawson RC, Krisht AF, Barrow DL, et al. **Treatment of experimental aneurysms using collagen-coated microcoils.** *Neurosurgery* 1995;36:133-140
2. Murayama Y, Tateshima S, Gonzalez NR, Vinuela F. **Matrix and bioabsorbable polymeric coils accelerate healing of intracranial aneurysms: long-term experimental study.** *Stroke* 2003;34:2031-2037
3. de Gast AN, Altes TA, Marx WF, et al. **Transforming growth factor beta-coated platinum coils for endovascular treatment of aneurysms: an animal study.** *Neurosurgery* 2001;49:690-696
4. Kallmes DF, Helm GA, Hudson SB, et al. **Histologic evaluation of platinum coil embolization in an aneurysm model in rabbits.** *Radiology* 1999;213:217-222
5. Böcher-Schwarz HG, Ringel K, Bohl J, et al. **Histological findings in coil-packed experimental aneurysms 3 months after embolization.** *Neurosurgery* 2002;50:379-385
6. Altes TA, Cloft HJ, Short JG, et al. **Creation of saccular aneurysms in the rabbit: A model suitable for testing endovascular devices.** *Am J Radiol* 2000;174:349-354
7. German W, Black S. **Experimental production of carotid aneurysms.** *N Engl J Med* 1954;3:463-468